SIW-Based Quad-Beam Leaky-Wave Antenna With Polarization Diversity for Four-Quadrant Scanning Applications

Anirban Sarkar, *Student Member, IEEE*, Soumava Mukherjee, *Member, IEEE*, Abhishek Sharma, *Student Member, IEEE*, Animesh Biswas, *Senior Member, IEEE*, and M. Jaleel Akhtar, *Senior Member, IEEE*

***Abstract*— A novel polarization diverse substrate integrated waveguide (SIW)-based leaky-wave antenna (LWA) is proposed for larger radiation coverage by frequency beam scanning in X-band. For feeding purpose, the SIW-based power divider, the directional coupler, and the 180° power splitter are used in the design. For radiation, +45°/−45° tilted slots are etched on top and bottom faces of the structure such that the radiated quad beam scans all the four quadrants. By varying the means of excitation at two input ports, multiple polarization states are realized. The antenna shows ±45° dual polarization (+45° and −45° are co-existing), horizontal and vertical polarization, and two types of circular dual-polarization (left handed and right handed simultaneously). The proposed antenna is capable of scanning in each of the four quadrants simultaneously with the scanning range of 62° having the maximum gain of 12.6 dBi and an improved cross-polarization level better than −20 dB. The quad beam covers overall scanning range of 248° with different polarization states. The S-parameters, radiation patterns, gain, and axial ratio are calculated and demonstrated. The proposed LWA shows desirable advantages, such as simultaneous four-quadrant frequency beam scanning having polarization diversity capabilities, which leads to a flexible design for practical utilization.**

***Index Terms*— Frequency beam-scanning, leaky-wave antenna (LWA), polarization diversity.**

I. Introduction

THE rapid growth in wireless services and other surveillance applications demands a new standard having maximum coverage area as well as good polarization reconfigurability. Since early days of mobile radio systems, various kinds of diversity mechanism in wireless communications have been studied [1]–[3]. In today's world, multiple antenna systems are very popular for modern wireless communication systems, where planar antennas or arrays are frequently used for polarization diversity [4]–[6]. Microstrip patch antenna is one of the choices [7], [8], but it is difficult to achieve right-hand circular polarization (RHCP) and left-hand CP (LHCP) reconfigurability [9]–[11]. The challenges here mainly lie in obtaining multilayer fabrication [12] and wide beam scanning range. Several patch element-based multiple polarization antennas have been proposed in past years. In [13], multibeam antenna having dual-orthogonal polarization property has been proposed, where lens array is used for angle diversity and antenna elements are designed such that they show polarization diversity. Longitudinal and transverse asymmetries are utilized in [14] to design periodic a leaky-wave antenna (LWA), where two orthogonal modes are generated simultaneously to achieve polarization diversity. In [15], a cavity backed reconfigurable array antenna has been designed where couplers, crossover, and delay lines are used for CP generation. However, the design of polarization reconfigurable antenna having excellent radiation coverage is still a challenging research area. It is to be noted, reconfigurable elements can sometimes be used in beam-scanning technology. However, it restricts the number of possible beam configurations with increased complexity especially when larger coverage area is needed. The LWA, which belongs to traveling wave antenna family, is a very good alternative in various applications like radar, satellite, and surveillance system for its frequency beam scanning capability with simpler feeding mechanism [16], [17]. Conventionally, the slotted metallic waveguide with transverse slot works as an LWA, which has frequency beam-scanning capability and orthogonal polarization. However, many modern wireless RF applications require compact system design involving dynamic polarization states. Hence, the metallic waveguide-based LWAs are not appropriate for this purpose.

For modern wireless applications, the compact antenna system using substrate integrated waveguide (SIW) technology has become quite popular in recent years because of its certain advantages such as lightweight, low loss, low cost, and ease of fabrication [18]–[23]. It is to be noted that, at millimeter wave frequencies (Ka-band and above), although the size of metallic waveguide becomes small, the SIW-based antennas are still preferred because of their easy integration with planar circuitry. To achieve CP, various SIW-based antennas have been designed and demonstrated in [24]–[26]. In [27], the TE_{20} mode of the SIW has been used to design dual-beam LWA for two-quadrant simultaneous frequency beam scanning. Several other dual-beam LWAs have been designed in past years for enhancing the beam scanning

Manuscript received November 1, 2017; revised April 12, 2018; accepted May 17, 2018. Date of publication May 23, 2018; date of current version August 2, 2018. *(Corresponding author: Anirban Sarkar.)*

A. Sarkar, A. Sharma, A. Biswas, and M. Jaleel Akhtar are with the Department of Electrical Engineering, IIT Kanpur, Kanpur 208016, India (e-mail: anirban.skr227@gmail.com).

S. Mukherjee is with the Department of Electrical Engineering, IIT Jodhpur, Jodhpur 342011, India.

Color versions of one or more of the figures in this paper are available online at http://ieeexplore.ieee.org.

Digital Object Identifier 10.1109/TAP.2018.2839887

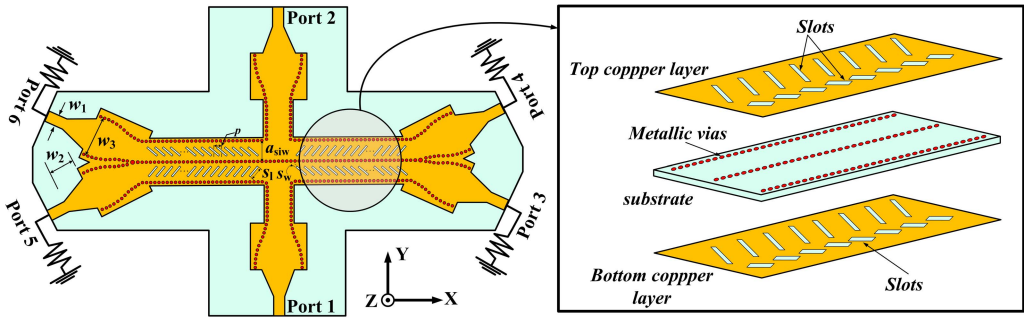

Fig. 1. Layout of the proposed antenna (top view), where the three layers are shown as magnified.

range [28]–[30]. In [31], a dual-polarized antenna has been realized by slotted postwall waveguide array, i.e., the SIW, where ±45° linear polarization is achieved on a single layered substrate. Finally, all the above-mentioned technologies are amalgamated and exploited in designing SIW-based LWAs for frequency beam scanning as well as polarization diversity applications. In [32], the half-mode SIW-based frequency beam-scanning antenna has been proposed. The antenna is capable to change its four states of polarization dynamically depending upon the mode of excitation. However, the single radiated beam in this case can scan only two quadrants with 30° scanning range in each. Recently, the composite right-handed (RH)/left-handed (LH) LWA [33], [34] has been proposed for full-space scanning, which covers six different polarization states [35]. It is to be noted that although the LWA presented in [35] shows some kind of polarization flexibility, it still uses a single radiated beam at a particular frequency in order to facilitate backfire to endfire scanning capabilities. At a fixed frequency, the single radiated main beam here scans only in either the second or first quadrant of the space depending upon LH or RH regions, respectively, with a cross polarization level in the order of −15 dB. Therefore, it can be inferred that most of the earlier proposed SIW-based leaky-wave structures have limited capability in order to facilitate polarization diversity with frequency beam scanning.

In this paper, an SIW-based LWA is proposed, which is capable to scan all the four quadrants simultaneously with multiple polarization states. Tilted radiating rectangular slots are etched suitably on top as well as at the bottom of the proposed structure to get full radiation coverage. Specifically, it has multiple polarization states ±45° linear dual polarization, X-polarization (horizontal), Y-polarization (vertical), and two CP. When excited at Port 1 or Port 2, ±45° or ∓45° LP radiation takes place. When Ports 1 and 2 are excited simultaneously and are in phase, the X-polarized wave will be generated. When Ports 1 and 2 are excited simultaneously but out of phase, Y-polarized wave will be produced. Moreover, when Ports 1 and 2 are excited by two equal amplitude with 90° phase difference signals simultaneously, CP is taken place. A Y-type 3-dB SIW power divider, directional coupler, and a 180° power splitter are incorporated with the feeding network. It should be pointed out that the proposed structure shows a significant four-quadrant overall scanning range of 248° (∼62° in each of the four quadrants) within the operating frequency band in contrast to single radiated beam used in [35]. Here, at a fixed frequency, four radiated main beams scan all the four

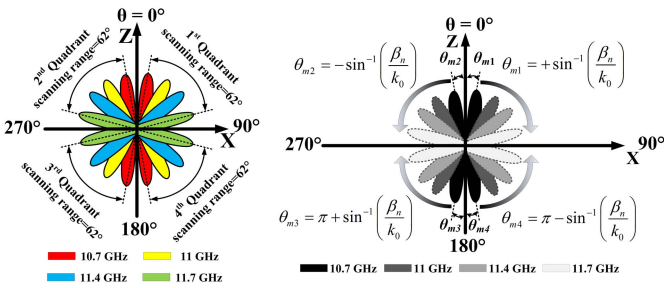

Fig. 2. (a) Layout of 248° four-quadrant radiation coverage by the proposed quad-beam LWA. (b) Working mechanism of four-quadrant scanning by the proposed structure.

quadrants simultaneously. Moreover, radiating slots are simple ±45° tilted rectangular shaped whose cross polarization level is better than −20 dB, which appears to be a good alternative to control the polarization states with better radiation properties than the earlier proposed SIW LWA's. To the best of our knowledge, such type of SIW-based LWA with polarization diversity has not been proposed earlier in literature.

This paper is organized by demonstrating about the antenna structure and operating principle in Section II, antenna design in Section III, and by discussing the results in Section IV. Finally, conclusion is drawn in Section V. The proposed antenna has quad-beam radiation pattern, where four quadrants can be scanned simultaneously with dynamic polarization compatibility.

II. Proposed Geometry and Operating Principle

A. Geometrical Layout

The top view of the proposed multiple polarization wide frequency beam scanning LWA is shown in Fig. 1, where the top layer, the substrate, and the bottom layer are shown in inset. The proposed six-port LWA is composed of a pair of front-to-front connected T-type SIW power dividers having appropriate matching network for microstrip to the SIW transition. It has six ports among which Ports 1 and 2 are used as input ports, keeping other output ports with 50 Ω matched termination. ±45° tilted slots are etched on both top and bottom layers of the structure so that the whole structure supports all kinds of polarization states with frequency beam scanning in all the four quadrants simultaneously as shown in Fig. 2(a) and (b). Periodicity of the slots are maintained by considering the homogeneity condition, i.e., $p < \lambda_0/4$. 36 slots are etched on each part ($\sim 5.6\lambda_0$) of the four sections

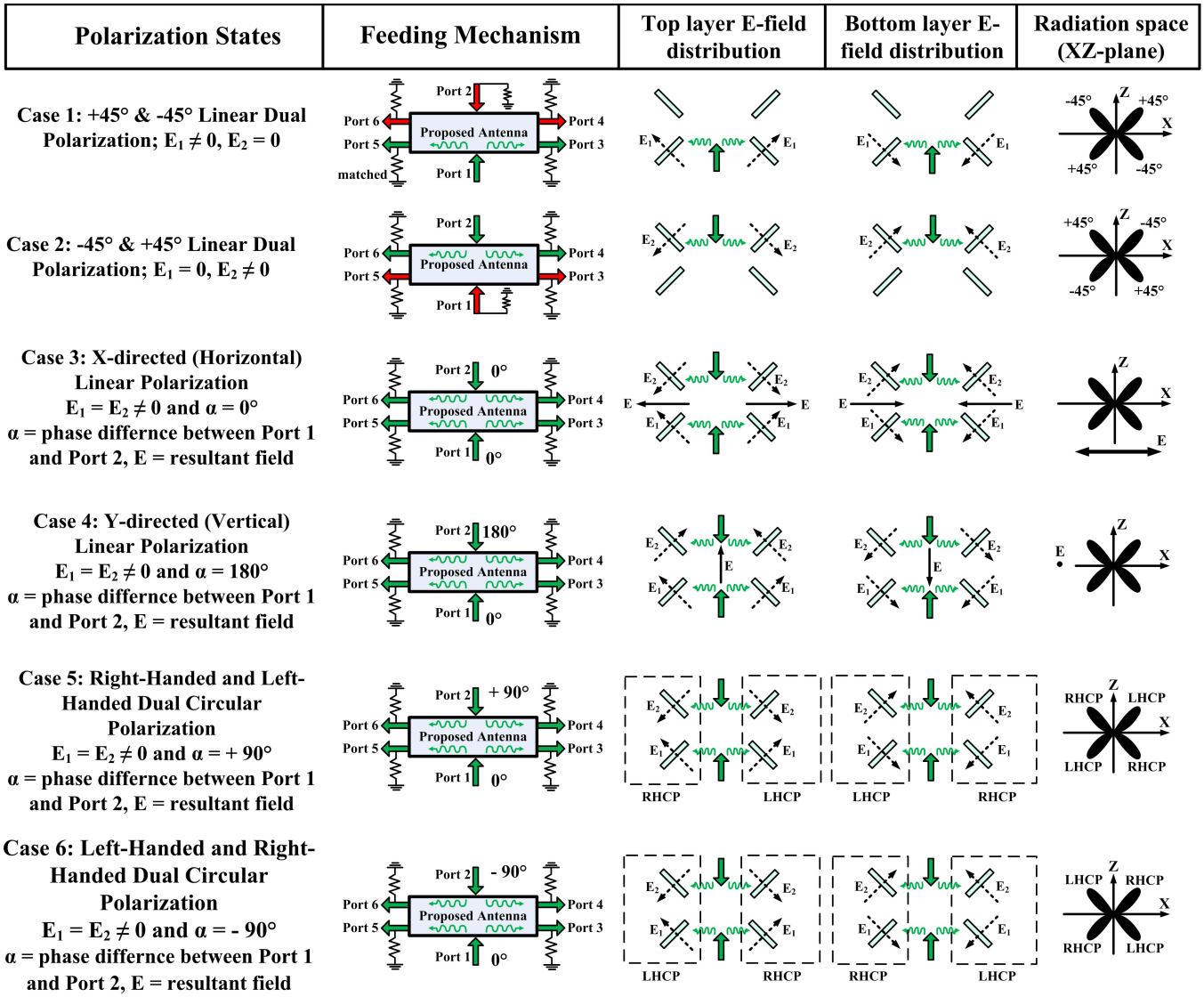

Fig. 3. Representation of different polarization states based on various feeding mechanisms and corresponding electric field vector orientation.

and the radiated main beam covers all of the four quadrants, where nth spatial harmonic phase constant is less than the free space wavenumber k_0, i.e., within the fast wave region. The center metallic via wall maintains good isolation between two SIW lines. A Y-type 3 dB SIW power divider, a 3-dB directional coupler with 90° phase difference between the output ports, and 180° power splitter are designed separately and utilized at the input ports of the antenna to get all the possible combinations of feeding signal for multiple polarization. Via walls are tapered suitably at the transition between tapered microstrips to the SIW for better impedance matching. The structure is fabricated on a substrate of Rogers RT/Duroid 5880 with a permittivity of 2.2, loss tangent of 0.0009, and a height of 1.57 mm. The diameter of via hole is kept 0.8 mm and intervia spacing is 1.5 mm. The other design parameters are $a_{\text{siw}} = 10.5$ mm, $S_l = 4.55$ mm, $S_w = 0.45$ mm, $p = 2.5$ mm, $w_1 = 5$ mm, $w_2 = 16$ mm, and $w_3 = 16.5$ mm.

B. Polarization Diversity

The operating principle of the LWA is shown in Fig. 3. By using an appropriate representation of electric field vector orientation into the radiating slots of the top and bottom planes, the polarization properties are systematically explained. The E-field vector at the bottom plane is opposite to the slots of the top plane as shown in Fig. 3. When the antenna is fed from Port 1, keeping other ports matched, the incident wave is divided into two parts and absorbed at Ports 3 and 5. Then, ±45° dual-LP radiation can be generated. Similarly, the same polarization in opposite direction can also be obtained if power is fed through Port 2. When Ports 1 and 2 are fed simultaneously with equal magnitude and in-phase signals, X-directed linear polarization (horizontal

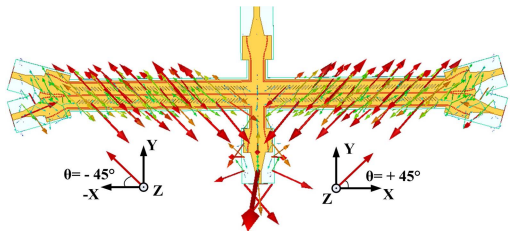

Fig. 4. Orientation of E-field vector for ±45° linear dual-polarization state.

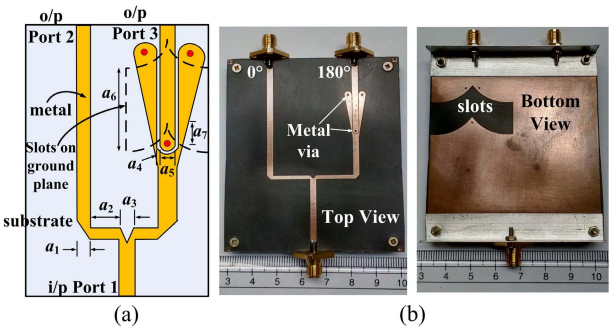

Fig. 5. Design of 180° power splitter. (a) Schematic and (b) top and bottom views of fabricated prototype. Optimized dimensions are (mm): $a_1 = 2.4$, $a_2 = 14.55$, $a_3 = 2.5$, $a_4 = 0.2$, $a_5 = 2.4$, $a_6 = 14$, and $a_7 = 2.4$.

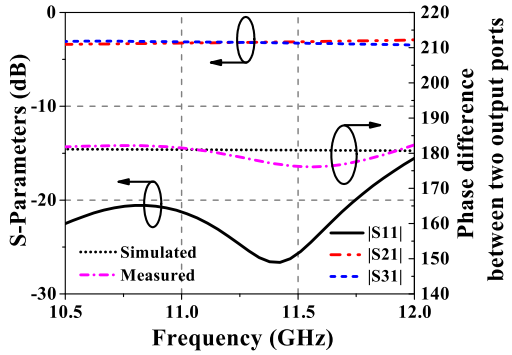

Fig. 6. S-parameter responses of the proposed 180° power splitter and phase variation between the output ports with frequency.

polarization) is obtained. From Fig. 3, it is clear that E is the resultant vector of the two input radiated electric field vector E_1 and E_2 and E is oriented in X-direction (either +X or −X). Y-directed polarization (vertical polarization) can be obtained if the input ports are fed by equal magnitude but 180° out-of-phase signals. Similarly, in this case, as shown in Fig. 3, it is clear that the resultant field is now oriented in Y-direction (either +Y or −Y). When the input ports are simultaneously fed by equal and 90° phase difference signals, RHCP and LHCP are formed and co-exist. The LHCP exists in the first and third quadrants of the visible space, i.e., diagonally, whereas RHCP is in the second and fourth quadrants. The polarization is reversed when input ports are fed by equal and −90° phase difference signals. To ensure the possible combinations of input power, external feeding circuits are used. A 3-dB power divider, directional coupler, and a novel 180° power splitter are designed, fabricated, and incorporated with the antenna for controlling polarization states. All the full wave simulations are carried out by Ansoft's High Frequency Structure Simulator software.

III. Antenna Design Procedure

Periodic LWAs are generally realized by incorporating periodic perturbations to the guided mode of the structure such that $n = -1$ floquet mode becomes fast and radiating in nature. The ±45° tilted slot is placed periodically in series on both sides of the structure with the periodicity p in such a manner that the scanning range of the LWA will be in the fast wave region within frequency range of 10.7–11.7 GHz. In this frequency range, the nth space harmonic phase constant (β_n) increases from zero to k_0. Moreover, the average cell size p must be substantially smaller than the guided wavelength λ_g to satisfy the homogeneity condition. In the fast wave region, β_n is less than the free space wavenumber, i.e., $|\beta_n| < k_0$ which is necessary radiation condition of LWA. The designed

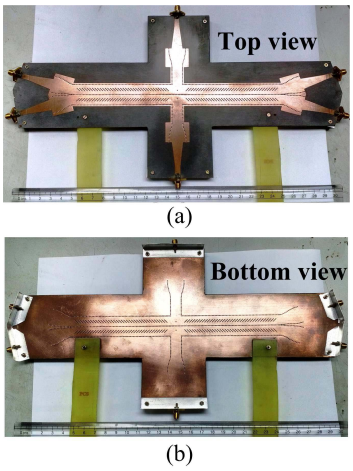

Fig. 7. Fabricated prototype of the proposed antenna. (a) Top plane. (b) Bottom plane.

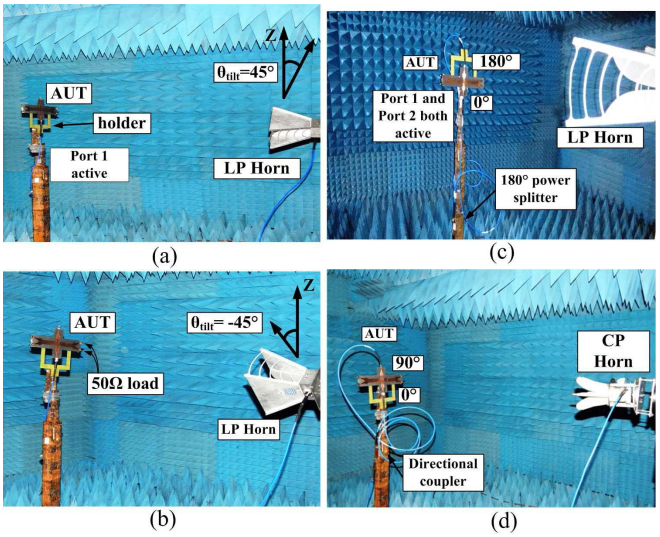

Fig. 8. Measurement setup of proposed antenna for different states of polarization. (a) +45° LP. (b) −45° LP. (c) Y-polarization. (d) CP (LHCP).

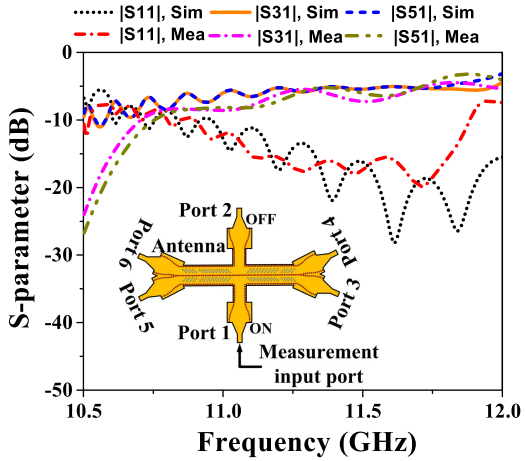

Fig. 9. Comparison of simulated and measured S-parameters for the linear dual-polarized LWA of Case 1.

LWA comprises of 36 unit cells and tapered microstrip line to tapered SIW transitions are used for impedance matching at all ports. The parameters w_2 and w_3 are optimized for the purpose of good impedance matching. The phase constant of the nth spatial harmonic β_n determines the direction of radiated main beam measured in all the four quadrants of visible space (1). Here, $n = -1$ space harmonic is responsible for radiation. The direction of maximum radiation (θ_m) can be calculated as [27], [36]

$$\beta_n = \cos^{-1}\left(\frac{1 - S_{11}S_{22} + S_{12}S_{21}}{2pS_{21}}\right) \tag{1}$$

and

$$\theta_{m1,2} = \pm\sin^{-1}\left(\frac{\beta_n}{k_0}\right) = \pm\sin^{-1}\left(\frac{\beta_0}{k_0} + \frac{n\lambda_0}{p}\right)$$
$$\theta_{m3,4} = \pi \pm \sin^{-1}\left(\frac{\beta_n}{k_0}\right) = \pi \pm \sin^{-1}\left(\frac{\beta_0}{k_0} + \frac{n\lambda_0}{p}\right) \tag{2}$$

where $\theta_{m1,2}$ represents the radiated beam direction in the first and second quadrants and $\theta_{m3,4}$ for the third and fourth quadrants, β_0 is the fundamental spatial harmonic, k_0 is the free space wavenumber, and p is the periodicity. Equation (2) shows that a full space scanning (0° to 360°) can be achieved if β_n varies with the range (0, k_0). To incorporate multiple polarization states with the proposed antenna, external circuits are used to control magnitude and phase of the input signal at the antenna. In Fig. 3, ±45° dual-LP radiation is shown and the simulated E-field vector distribution of top plane is shown in Fig. 4. In measurement, the linearly polarized horn antenna is rotated by ±45° to get a full coverage with radiated dual-LP quad beam radiation. This is shown later in Fig. 8. Next, a 3 dB SIW-based Y-type power divider is exploited for design purpose to feed the antenna with equal magnitude and in-phase signals resulting X-directed LP [37]. A novel 180° power splitter having two equal magnitude but 180° out-of-phase signals is designed, which is used to generate Y-directed LP. The schematic of the power splitter and its fabricated prototype are shown in Fig. 5(a) and (b). The power splitter has good amplitude imbalance of ∼0.4 dB and a measured maximum phase variation of ±6° between output ports. The responses of the 180° power splitter is shown in Fig. 6, where the amplitude as well as phase imbalance are obtained. For simulation purpose, equiamplitude signals are fed directly with suitable phase value at the input ports and to reduce the simulation time, feeding circuits are not simulated with the whole antenna. To achieve dual-CP, a 3-dB hybrid directional coupler is designed separately to feed the antenna [38]. As top and bottom planes of SIW have 180° phase shift, the first and third quadrants are with the same LHCP and the second and fourth quadrants are in RHCP. A dual-circular polarized horn is used for measurement purpose. S-parameters, radiation pattern, and axial ratios (ARs) are calculated and described in Section IV.

IV. Results and Discussions

To experimentally validate the design concept and methodology, the proposed antenna is fabricated on single layer substrate by normal PCB fabrication process. The fabricated prototype is shown in Fig. 7. The radiation properties of the antenna are measured in anechoic chamber using a setup shown in Fig. 8. Comparison of simulated and measured reflection coefficients for ±45° linear dual polarization (Case 1) are shown in Fig. 9 which shows a good matching. The antenna is working within the frequency range of 10.7–11.7 GHz (| $S11$ |≤ −10 dB). We have performed

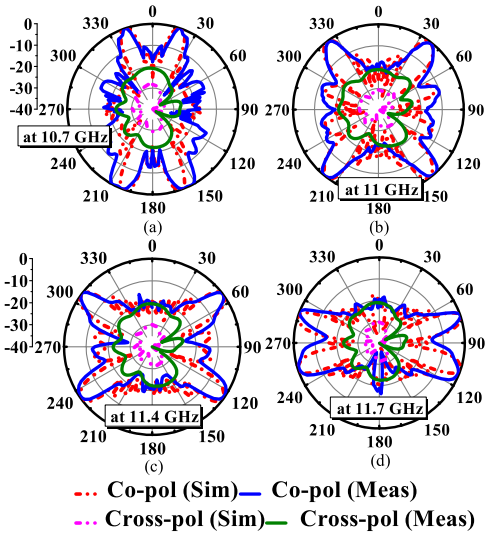

Fig. 10. Comparison of simulated and measured normalized radiation patters in the XZ plane for Case 1 at different frequencies. (a) 10.7 GHz. (b) 11 GHz. (c) 11.4 GHz. (d) 11.7 GHz.

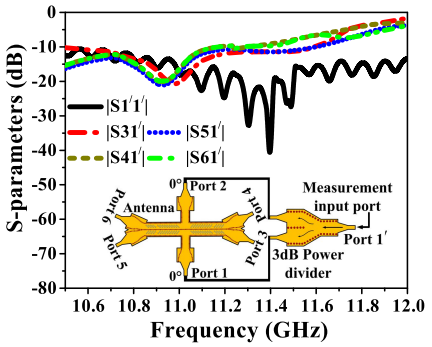

Fig. 11. Measured S-parameter responses for the X-polarized LWA (Case 3).

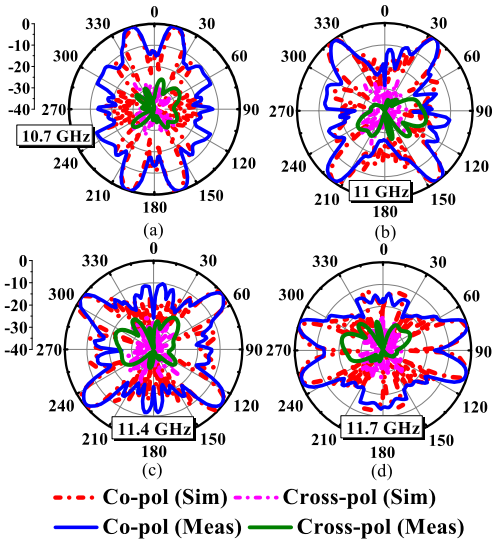

Fig. 12. Comparison of simulated and measured normalized radiation patters in the XZ plane for X-polarized LWA (Case 3) at different frequencies. (a) 10.7 GHz. (b) 11 GHz. (c) 11.4 GHz. (d) 11.7 GHz.

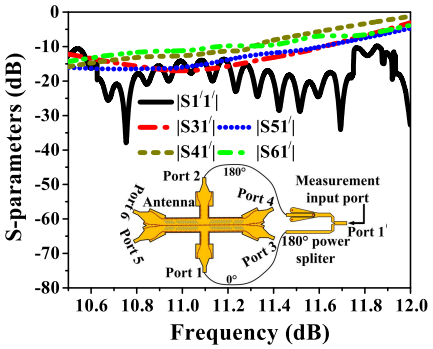

Fig. 13. Measured S-parameter responses for the Y-polarized LWA (Case 4).

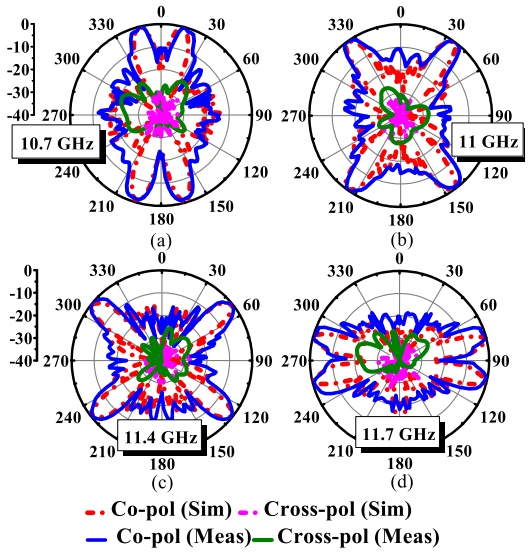

Fig. 14. Comparison of simulated and measured normalized radiation patters in the XZ plane for Y-polarized LWA (Case 4) at different frequencies. (a) 10.7 GHz. (b) 11 GHz. (c) 11.4 GHz. (d) 11.7 GHz.

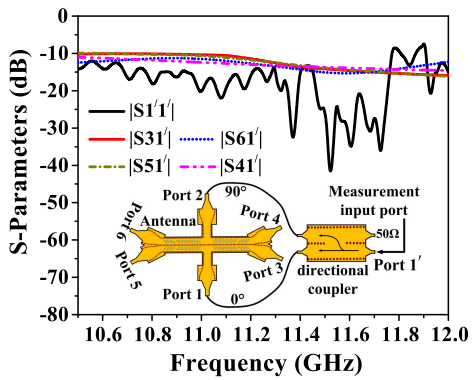

Fig. 15. Variation of measured S-parameters of LHCP–RHCP dual-polarized LWA with frequencies where only three parameters are shown (Case 5).

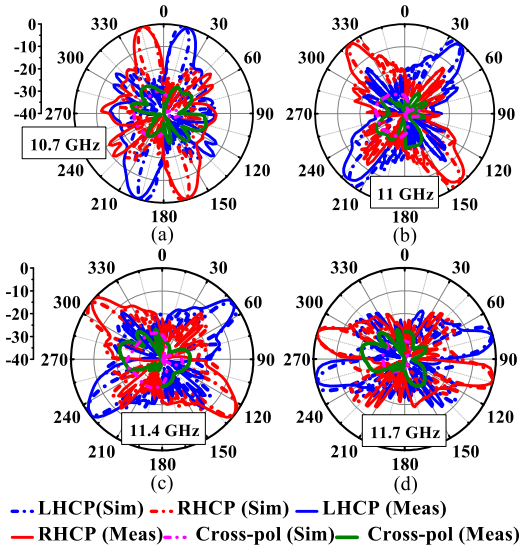

Fig. 16. Comparison of simulated and measured normalized radiation patters in the XZ plane for RHCP–LHCP dual-polarized LWA (Case 5) at different frequencies. (a) 10.7 GHz. (b) 11 GHz. (c) 11.4 GHz. (d) 11.7 GHz.

the S-parameter measurements using two-port vector network analyzer. The calculated S-parameters in Fig. 9 are corresponding to the antenna ports given in inset, where Port 1 is acting as a measurement input port. However, when we use external feeding circuitry, such as power divider, 180° power splitter, and directional coupler, the measurement input port is then shifted to input port of feeding network, which is designated as Port 1′ as shown in inset of Figs. 11, 13, and 15, respectively. This incorporates the losses due to the feeding network in the measured data of S-parameters. The normalized simulated and measured radiation patterns in XZ-plane are shown in Fig. 10. Here, the proposed antenna scans a range of 52° in each of the four quadrants (from 20° to 72° for the first quadrant, −20° to −72° for the second quadrant, 200° to 252° for the third quadrant, and 160° to 108° for the fourth quadrant). The obtained values of measured peak gains are 8.73, 10.06, 11.64, and 11.68 dBi at 10.7, 11, 11.4, and 11.7 GHz, respectively. The measured minimum cross-polar levels in the radiated main beam directions are achieved as −20.74 dB at 10.7 GHz, −20.19 dB at 11 GHz, −20.44 dB at 11.4 GHz, and −21.13 dB at 11.7 GHz. Results for Case 2 are not presented as it is reverse case of Case 1, i.e., signal is fed at Port 2. The similar scanning range is covered by the antenna when equimagnitude and equiphase signals are fed at the input to achieve X-directed polarization (Case 3). The S-parameters are shown in Fig. 11 and the setup is shown in inset. The normalized radiation patterns in XZ-plane are shown in Fig. 12, where the measured radiated beam scans each of the four quadrants with frequencies having the scanning range of 62° (from 14° to 76° for the first quadrant, −16° to −78° for the second quadrant, 198° to 260° for the third quadrant, and 162° to 100° for the fourth quadrant). The obtained values of measured peak gains for this case are 9.75, 11.08, 11.94, and 11.98 dBi at 10.7, 11, 11.4, and 11.7 GHz, respectively. The measured minimum cross-polar levels in the radiated main beam directions are achieved as −25.56 dB at 10.7 GHz, −20.73 dB at 11 GHz, −21.64 dB at 11.4 GHz, and −20.74 dB at 11.7 GHz.

A similar procedure has been adopted for the measurement of S-parameter responses for Y-directed polarization (Case 4) as shown in Fig. 13 and the measurement setup layout is shown in inset. The normalized measured and simulated radiation patterns are compared at different frequencies for Y-directed polarization and shown in Fig. 14. It shows a scanning range of 60° (from 14° to 74° for the first quadrant, −14° to −74° for the second quadrant, 196° to 256° for the third quadrant,

TABLE I
PERFORMANCE COMPARISON OF ALL POLARIZATION STATES. BW = BANDWIDTH

Polarization states	Quadrant-wise scanning range within frequency range 10.7-11.7 GHz	BW (%)	SLL (dB)	Minimum cross-polar level (dB)	Achieved maximum gain (dBi)
Case 1 and 2: $\pm 45°$ and $\mp 45°$ linear dual polarization	1^{st} quadrant: 52° (20° to 72°); 2^{nd} quadrant: 52° (-20° to -72°); 3^{rd} quadrant: 52° (200° to 252°); 4^{th} quadrant: 52° (160° to 108°)	7.82	<10 dB	-20.74 @ 10.7 GHz; -20.19 @ 11 GHz; -20.44 @ 11.4 GHz; -21.13 @ 11.7 GHz	11.68
Case 3: X-directed (Horizontal) linear polarization	1^{st} quadrant: 62° (14° to 76°); 2^{nd} quadrant: 62° (-16° to -78°); 3^{rd} quadrant: 62° (198° to 260°); 4^{th} quadrant: 62° (162° to 100°)	8.92	<10 dB	-25.56 @ 10.7 GHz; -20.73 @ 11 GHz; -21.64 @ 11.4 GHz; -20.74 @ 11.7 GHz	11.98
Case 4: Y-directed (Vertical) linear polarization	1^{st} quadrant: 60° (14° to 74°); 2^{nd} quadrant: 60° (-14° to -74°); 3^{rd} quadrant: 60° (196° to 256°); 4^{th} quadrant: 60° (164° to 104°)	8.92	<10 dB	-25.21 @ 10.7 GHz; -26.35 @ 11 GHz; -21.24 @ 11.4 GHz; -20.44 @ 11.7 GHz	12.43
Case 5/6: Right handed and Left handed dual circular polarization	LHCP/RHCP in 1^{st} quadrant: 60° (16° to 76°); RHCP/LHCP in 2^{nd} quadrant: 60° (-14° to -74°); LHCP/RHCP in 3^{rd} quadrant: 58° (198° to 256°); RHCP/LHCP in 4^{th} quadrant: 60° (164° to 104°)	8.92	<10 dB	-21.5 @ 10.7 GHz; -24.5 @ 11 GHz; -20.73 @ 11.4 GHz; -20.74 @ 11.7 GHz	12.14

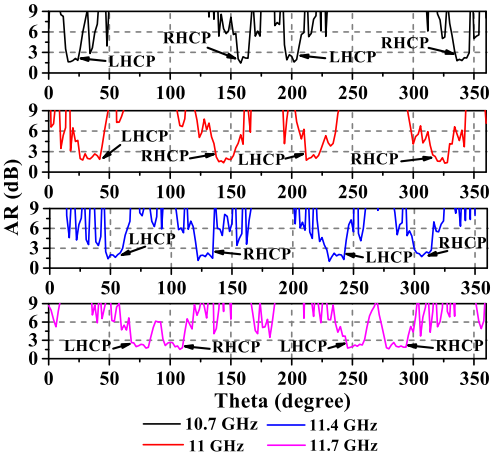

Fig. 17. AR at different frequencies for LHCP–RHCP dual-polarized LWA (Case 5).

and 164° to 104° for the fourth quadrant) in each of the four quadrants. The obtained values of measured peak gains for this case are 9.01, 10.34, 12.39, and 12.43 dBi at 10.7, 11, 11.4, and 11.7 GHz, respectively. The measured minimum cross-polar levels in the radiated main beam directions are achieved as −25.21 dB at 10.7 GHz, −26.35 dB at 11 GHz, −21.24 dB at 11.4 GHz, and −20.44 dB at 11.7 GHz. Finally, the CP property of the antenna with suitable setup is investigated and discussed here. An SIW hybrid directional coupler is used to excite the proposed antenna with two orthogonally polarized input signals. The whole setup is shown in the inset of Fig. 15. If the structure is fed according to the layout shown in Fig. 3, the radiating slots of right side top plane and left side bottom plane from the center of the antenna show LHCP. On the other hand, for the same configuration, the radiating slots of left side top plane and right side bottom plane show RHCP. Thus, dual CP is achieved (Case 5). The polarization is reversed if the input signals of the antenna are interchanged (Case 6). The S-parameter responses for dual CP are shown in Fig. 15. The antenna measurement setup is shown in inset of Fig. 15, where the antenna is fed by external feeding circuit. The measured operating bandwidth is achieved from 10.7–11.7 GHz (below −10 dB). The simulated normalized radiation patterns are compared with the measured responses shown in Fig. 16. It shows an LHCP scanning range of 60° and 58° for the first quadrant (from 16° to 76°) and the third quadrant (from 198° to 256°), respectively. The RHCP scanning range is achieved as 60° for the second quadrant (from −14° to −74°) and the fourth quadrant (164° to 104°). The obtained values of measured peak gains for this case are 9.19, 10.52, 12.09, and 12.14 dBi at 10.7, 11, 11.4, and 11.7 GHz, respectively. The achieved value of maximum peak gain is 12.6 dBi at 11.5 GHz. The measured minimum cross-polar levels in the radiated main beam directions are achieved as −21.5 dB at 10.7 GHz, −24.5 dB at 11 GHz, −20.73 dB at 11.4 GHz, and −20.74 dB at 11.7 GHz. At the time of AR estimation for different frequencies, the horn antenna has been rotated at corresponding desired angles. Four different frequencies are studied and the results are plotted in Fig. 17. It is found that AR is always better than 3 dB at desired direction. It is clear that, at 10.7 GHz, the antenna is showing dual polarization simultaneously at angle 16° and 198° for LHCP and 164° and 346° for RHCP. Similarly, other frequency points are easily predictable from the same figure. All the measurements have been performed in anechoic chamber maintaining the far-field boundary conditions. A dual-polarized standard horn antenna is used during measurement of CP. The measured performances are well matched with the simulated results. The little discrepancy is observed in measured results due to the imperfections of coupler performances, power divider responses, cable loss, and fabrication tolerance. The sidelobe level is better than 10 dB for both the LHCP and RHCP radiation patterns. All the radiation patterns are plotted in XZ-plane. A detailed comparison explaining all the performances of various polarization states is shown in Table I. The proposed antenna is useful for multibeam antenna applications and advantageous in terms of radiated beam scanning with polarization flexibility as it scans all of the four quadrants simultaneously. The antenna is also planar and structurally simple, since the basic SIW geometry is exploited here with simpler shape of radiating slots.

V. Conclusion

In this paper, an SIW-based quad-beam frequency beam scanning LWA with polarization diversity has been proposed and demonstrated. Depending upon the excitation profile, the antenna has the ability to change its multiple polarization states which support a pair of linear dual polarizations, horizontal-directed LP, vertical-directed LP, and a pair of circular dual polarizations. The antenna is working within the frequency band of 10.7–11.7 GHz having a maximum scanning range of 62° in each of the four quadrants and a maximum achieved peak gain of 12.6 dBi. Good cross-polarization level is observed during measurements. Along with the wide range of four-quadrant scanning coverage of 248° for radio and mobile communications, the proposed prototype is a single layered structure with simple geometry. The proposed antenna can potentially be used for base station and various wireless communication applications requiring polarization diversity.

References

[1] W. C. Jakes, Ed., *Microwave Mobile Communications*. Piscataway, NJ, USA: IEEE Press, 1994.

[2] R. G. Vaughan, "Polarization diversity in mobile communications," *IEEE Trans. Veh. Technol.*, vol. 39, no. 3, pp. 177–186, Aug. 1990.

[3] C.-J. Ahn, "Maritime VHF communications with polarization diversity over a Rician channel," IEICE, Tech. Rep. CS2010-109, Mar. 2011, pp. 219–222.

[4] W. L. Stutzman, J. H. Reed, C. B. Dietrich, B. K Kim, D. G. Sweeney, "Recent results from smart antenna experiments-base station and hand-held terminals," in *Proc. IEEE Radio Wireless Conf. (RAWCON)*, Denver, CO, USA, Sep. 2000, pp. 139–142.

[5] B. S. Collins, "Polarization diversity antennas for compact base stations," *Microw. J.*, vol. 43, pp. 76–88, Jan. 2000.

[6] C. Beckman and U. Wahlberg, "Antenna systems for polarization diversity," *Microw. J*, vol. 40, no. 5, pp. 330–334, May 1997.

[7] M. Elhefnawy and W. Ismail, "A microstrip antenna array for indoor wireless dynamic environments," *IEEE Trans. Antennas Propag.*, vol. 57, no. 12, pp. 3998–4002, Dec. 2009.

[8] W. Cao, B. Zhang, A. Liu, T. Yu, D. Guo, and K. Pan, "A reconfigurable microstrip antenna with radiation pattern selectivity and polarization diversity," *IEEE Antennas Wireless Propag. Lett.*, vol. 11, pp. 453–456, 2012.

[9] Y. J. Sung, T. U. Jang, and Y. S. Kim, "A reconfigurable microstrip antenna for switchable polarization," *IEEE Microw. Wireless Compon. Lett.*, vol. 14, no. 11, pp. 534–536, Nov. 2004.

[10] K. Chung, Y. Nam, T. Yun, and J. Choi, "Reconfigurable microstrip patch antenna with switchable polarization," *ETRI J.*, vol. 28, no. 3, pp. 379–382, 2006.

[11] F. Yang and Y. Rahmat-Samii, "A reconfigurable patch antenna using switchable slots for circular polarization diversity," *IEEE Microw. Wireless Compon. Lett.*, vol. 12, no. 3, pp. 96–98, Mar. 2002.

[12] T. Lambard, O. Lafond, M. Himdi, H. Jeuland, S. Bolioli, and L. Le Coq, "Ka-band phased array antenna for high-data-rate SATCOM," *IEEE Antennas Wireless Propag. Lett.*, vol. 11, pp. 256–259, 2012.

[13] D. Popovic and Z. Popovic, "Multibeam antennas with polarization and angle diversity," *IEEE Trans. Antennas Propag.*, vol. 50, no. 5, pp. 651–657, May 2002.

[14] A. Al-Bassam, S. Otto, D. Heberling, and C. Caloz, "Broadside dual-channel orthogonal-polarization radiation using a double-asymmetric periodic leaky-wave antenna," *IEEE Trans. Antennas Propag.*, vol. 65, no. 6, pp. 2855–2864, Jun. 2017.

[15] S. Karamzadeh, V. Rafii, H. Saygin, and M. Kartal, "Polarisation diversity cavity back reconfigurable array antenna for C-band application," *IET Microw., Antennas Propag.*, vol. 10, no. 9, pp. 955–960, 2016.

[16] D. R. Jackson and A. A. Oliner, *Modern Antenna Handbook*. Hoboken, NJ, USA: Wiley, 2008.

[17] L. O. Goldstone and A. A. Oliner, "Leaky-wave antennas I: Rectangular waveguides," *IRE Trans. Antennas Propag.*, vol. 7, no. 4, pp. 307–319, Oct. 1959.

[18] D. Deslandes and K. Wu, "Single-substrate integration technique of planar circuits and waveguide filters," *IEEE Trans. Microw. Theory Techn.*, vol. 51, no. 2, pp. 593–596, Feb. 2003.

[19] D. Deslandes and K. Wu, "Integrated microstrip and rectangular waveguide in planar form," *IEEE Microw. Wireless Compon. Lett.*, vol. 11, no. 2, pp. 68–70, Feb. 2001.

[20] L. Yan, W. Hong, G. Hua, J. Chen, K. Wu, and T. J. Cui, "Simulation and experiment on SIW slot array antennas," *IEEE Microw. Wireless Compon. Lett.*, vol. 14, no. 9, pp. 446–448, Sep. 2004.

[21] W. Hong *et al.*, "SIW-like guided wave structures and applications," *IEICE Trans. Electron.*, vol. E92.C, no. 9, pp. 1111–1123, Sep. 2009.

[22] T.-M. Shen, C.-F. Chen, T.-Y. Huang, and R.-B. Wu, "Design of vertically stacked waveguide filters in LTCC," *IEEE Trans. Microw. Theory Techn.*, vol. 55, no. 8, pp. 1771–1779, Aug. 2008.

[23] Y. D. Dong, T. Yang, and T. Itoh, "Substrate integrated waveguide loaded by complementary split-ring resonators and its applications to miniaturized waveguide filters," *IEEE Trans. Microw. Theory Techn.*, vol. 57, no. 9, pp. 2211–2223, Sep. 2009.

[24] Z. Chen, W. Hong, Z. Kuai, J. Chen, and K. Wu, "Circularly polarized slot array antenna based on substrate integrated waveguide," in *Proc. Int. Conf. Microw. Millim. Wave Technol.*, Nanjing, China, Apr. 2008, pp. 1066–1069.

[25] P. Chen, W. Hong, Z. Kuai, and J. Xu, "A substrate integrated waveguide circular polarized slot radiator and its linear array," *IEEE Antennas Wireless Propag. Lett.*, vol. 8, pp. 120–123, 2009.

[26] D. Kim, J. W. Lee, C. S. Cho, and T. K. Lee, "X-band circular ring-slot antenna embedded in single-layered SIW for circular polarisation," *Electron. Lett.*, vol. 45, no. 13, pp. 668–669, Jun. 2009.

[27] A. Sarkar, A. Sharma, M. Adhikary, A. Biswas, and M. J. Akhtar, "Bi-directional siw leaky-wave antenna using TE_{20} mode for frequency beam scanning," *Electron. Lett.*, vol. 53, no. 15, pp. 1017–1019, Jul. 2017.

[28] C. Luxey and J.-M. Latheurte, "Simple design of dual-beam leaky-wave antennas in microstrips," *IEE Proc.-Microw., Antennas Propag.*, vol. 144, no. 6, pp. 397–402, Dec. 1997.

[29] T.-L. Chen and Y.-D. Lin, "Dual-beam microstrip leaky-wave array excited by aperture-coupling method," *IEEE Trans. Antennas Propag.*, vol. 51, no. 9, pp. 2496–2498, Sep. 2003.

[30] C.-J. Wang, C. F. Jou, and J.-J. Wu, "A novel two-beam scanning active leaky-wave antenna," *IEEE Trans. Antennas Propag.*, vol. 47, no. 8, pp. 1314–1317, Aug. 1999.

[31] S. Park, Y. Okajima, J. Hirokawa, and M. Ando, "A slotted post-wall waveguide array with interdigital structure for 45° linear and dual polarization," *IEEE Trans. Antennas Propag.*, vol. 53, no. 9, pp. 2865–2871, Sep. 2005.

[32] Y. J. Cheng, W. Hong, and K. Wu, "Millimeter-wave half mode substrate integrated waveguide frequency scanning antenna with quadri-polarization," *IEEE Trans. Antennas Propag.*, vol. 58, no. 6, pp. 1848–1855, Jun. 2010.

[33] C. Caloz and T. Itoh, *Electromagnetic Metamaterials: Transmission Line Theory and Microwave Applications*. Hoboken, NJ, USA: Wiley, 2005.

[34] A. Sarkar, M. Adhikary, A. Sharma, A. Biswas, M. J. Akhtar, and Z. Hu, "Composite right/left-handed based compact and high gain leaky-wave antenna using complementary spiral resonator on HMSIW for Ku band applications," *IET Microw., Antennas Propag.*, vol. 12, no. 8, pp. 1310–1315, Jul. 2018. [Online]. Available: http://digital-library.theiet.org/content/journals/10.1049/iet-map.2017.0478

[35] Y. D. Dong and T. Itoh, "Substrate integrated composite right-/left-handed leaky-wave structure for polarization-flexible antenna application," *IEEE Trans. Antennas Propag.*, vol. 60, no. 2, pp. 760–771, Feb. 2012.

[36] C. Caloz, D. R. Jackson, and T. Itoh, *Frontiers in Antennas*, F. B. Gross, Ed. New York, NY, USA: McGraw-Hill, 2011.

[37] S. Datta, S. Mukherjee, and A. Biswas, "Design of broadband power divider based on substrate-integrated waveguide technology," in *Proc. Appl. Electromagn. Conf. (AEMC)*, Bhubaneswar, India, 2015, pp. 1–2.

[38] Z. C. Hao, W. Hong, J. X. Chen, H. X. Zhou, and K. Wu, "Single-layer substrate integrated waveguide directional couplers," *IEE Proc.-Microw., Antennas Propag.*, vol. 153, no. 5, pp. 426–431, Oct. 2006.

Anirban Sarkar (S'14), photograph and biography not available at the time of publication.

Soumava Mukherjee (S'11–M'17), photograph and biography not available at the time of publication.

Abhishek Sharma (S'13), photograph and biography not available at the time of publication.

Animesh Biswas (SM'96), photograph and biography not available at the time of publication.

M. Jaleel Akhtar (S'99–M'03–SM'09), photograph and biography not available at the time of publication.